

## Excited-State Photophysics and Dynamics of a Hemicyanine Dye in AOT Reverse Micelles

Jiho Kim and Minyung Lee\*

Department of Chemistry, Ewha Womans University, Seoul 120-750, Korea

Received: October 26, 1998; In Final Form: March 1, 1999

The internal rotation of a photoexcited hemicyanine dye, *trans*-4-[4-(dimethylamino)-styryl]-1-methylpyridinium iodide (DASPI), was investigated in water-containing reverse micelles. The rate constants for the twisting motion were obtained from the measured fluorescence lifetimes in various sizes of water nanoclusters (ca. 0.6–5.6 nm in radius) prepared from sodium bis(2-ethylhexyl) sulfosuccinate (AOT)–alkane–water solutions by changing the molar ratio of water/AOT. It was observed that the fluorescence lifetime of DASPI in the water pool formed by the reverse micelle markedly increases as the nanocluster size decreases, implying that the excited-state twisting motion is significantly influenced by the microstructure of the reverse micelle. An endeavor was made to relate the rate process for internal rotation to water pool characteristics such as polarity and viscosity.

### Introduction

The photophysics and photochemistry of *trans*-4-[4-(dimethylamino)-styryl]-1-methylpyridinium iodide (DASPI), a useful fluorescence probe, have been subjected to intensive studies, owing to its many interesting properties.<sup>1</sup> Upon photoexcitation, the molecule undergoes internal rotation that leads to the twisted intramolecular charge transfer (TICT) state.<sup>1,2</sup> As shown in Figure 1, the rotamerism process can take place via several pathways around three single bonds as well as one double bond, resulting in a very small fluorescence quantum yield in solution. Its fluorescence quantum yield strongly depends on solvent nature such as polarity and viscosity.<sup>3</sup> Recent direct time-resolved studies for the molecule in a low-temperature ethanol solution<sup>2</sup> and in DNA<sup>4</sup> verified experimentally that the internal twisting motion is responsible for the fast radiationless decay. It is not an easy matter to extract all the rate constants by simply measuring the fluorescence quantum yield or the excited-state lifetimes of the molecule because there are many isomerism processes involved in the excited state of DASPI. However, recent theoretical and experimental studies reveal a much simplified picture of the photophysics of DASPI. The essential results that are arranged at our disposal can be summarized as follows.<sup>1–5</sup>

(1) Photoexcitation induces the internal twisting motion that leads to several TICT states. Unlike other molecules having a TICT state, no dual fluorescence was observed in the emission spectra. Therefore, it was concluded that the TICT states are nonfluorescing, and thus, its fluorescence occurs only from the non-TICT state.

(2) The *trans*–*cis* isomerization (rotation of  $\phi_3$ ) is unlikely in the excited state because a very low isomerization yield (<1%) was observed.

(3) Twisting around  $\phi_1$  that involves the rotation of the dimethylamino group is unfavorable because the TICT state lies at higher energy.

(4) There exists a potential barrier for twisting of the methylpyridinium ring ( $\phi_4$ ). The barrier height is higher than

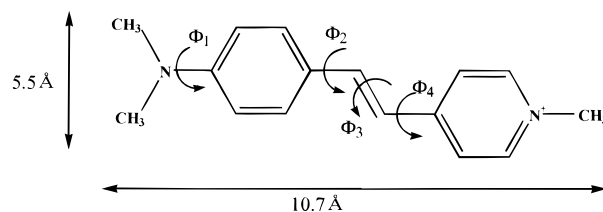


**Figure 1.** Molecular structure of *trans*-4-[4-(dimethylamino)-styryl]-1-methylpyridinium iodide (DASPI). Definition for the internal twisting angles was adopted from ref 1.

the thermal energy at room temperature. However, the result was only drawn from a calculation, and no experimental evidence has been reported yet.

(5) In the excited-state potential surface for the rotation through  $\phi_2$ , the barrier height depends on solvent polarity. The increase of solvent polarity lowers the barrier height. In aqueous solution, it becomes barrierless.

One notable feature of the above-mentioned results is that the internal rotation of the aniline moiety ( $\phi_2$ ) is mostly responsible for the efficient deactivation process of the electronically excited DASPI in aqueous solution.

There have been many studies of the photophysical properties of organic or biological molecules in water pools contained in reverse micelles. Surprisingly, to our knowledge, there is no systematic study of the excited-state twisting dynamics of any molecular system in reverse micelles. The purpose of this report is to study the internal twisting dynamics of DASPI in nanometer-sized reverse micelles, the photophysical property of which has been well characterized in bulk. The microemulsion of water is usually prepared by addition of a small amount of water to surfactants that form reverse micelles in a hydrocarbon solvent. Owing to the structure of the reverse micellar system, there is at least one stringent requirement for the probe molecule to be found inside the reverse micelle: The solubility should be high in water and low in hydrocarbon solvents.<sup>6</sup> DASPI is an ideal molecule for this purpose. For the surfactant, aerosol OT (sodium bis(2-ethylhexyl) sulfosuccinate, AOT) was chosen because it is known to provide the spherical shape of a water pool having the dimensions of nanometers. In *n*-heptane,

\* To whom correspondence should be addressed. Phone: 82-2-3277-2383. Fax: 82-2-3277-2384. E-mail: mylee@mm.ewha.ac.kr.

the radius of such a water pool is about  $2w$  (in angstroms) in which  $w$  is the number ratio of the water to the surfactant molecules.<sup>7</sup> Since the inside of the reverse micelle is charged, the droplet consists of two different types of water called the bound and the free water. In other words, the outside of the water droplet is less mobile in comparison with the inner side because of the negative charge of the surfactant. One piece of experimental evidence for this is the huge difference in the solvent relaxation time of the bound and the free water: The former is about 10 ns, and the latter has been identified as 10 ps.<sup>8</sup> These values are much larger than the solvent relaxation time of liquid water, which has been reported as subpicoseconds.<sup>9</sup>

By using time-resolved fluorescence spectroscopy, we investigated the photoinduced dynamics of DASPI in AOT reverse micelles that provide a spherical nanoreactor. Various sizes of water nanoclusters were prepared from AOT-*n*-heptane-water solution. When the molar ratio of water/AOT is changed, the nanocluster size of the radius was varied from 0.6 to 5.6 nm. An important finding of this work is that the luminescence intensity of DASPI in a water pool, decaying nonexponentially, depends critically on the reverse micelle size. The rate constants for the internal rotation were obtained from the measured decay times, and a phenomenological description was made on the rate processes in terms of the physical properties of the reverse micelle such as polarity and viscosity.

### Experimental Section

The fluorescence lifetimes were measured by using the time-correlated single-photon counting (TCSPC) system. The excitation light source was a picosecond Nd:YLF laser (Lightwave Electronics 130) operating at 100 MHz. Its pulse width was measured to be ca. 15 ps by a homemade scanning autocorrelator. The average power was routinely about 250 mW. The fundamental output (1047 nm) was frequency-doubled in a KTP crystal by type II phase-matching. The TCSPC electronics consist of a time-to-amplitude converter (Oxford TC864), two picotiming discriminators (Ortec 9307), a nanosecond delay (Ortec 425A), and a dual channel photon counter (Ortec 994). The second harmonic beam was separated from the fundamental by a dichroic beam splitter. The fundamental was used as the trigger pulse and the second harmonic signal as the excitation pulse. The trigger pulse was detected by an InGaAs fast photodiode (Electro-Optic Technology ET 3000) and amplified by a preamplifier (Ortec VT120C). The signal was divided by a BNC T-connector, one being sent to a 400 MHz digital oscilloscope (LeCroy 9310A) for pulse-train monitoring and the other to the picotiming discriminator for triggering. The excitation beam (523.5 nm) was oriented to the vertical polarization using a half-wave plate. The remnant fundamental was further removed by placing a Schott KG 3 filter in front of the sample cell. The fluorescence from the sample by excitation at 523.5 nm was collected with a lens and dispersed in a 27.5 cm focal length monochromator (ARC SP250). A visible sheet polarizer was placed in front of the monochromator for magic angle detection (54.7°). The excitation beam was blocked by a 560 nm cutoff filter. The monochromator was always set at the fluorescence maximum for detection. The fluorescence signal was detected by a microchannel plate tube PMT (Hamamatsu 3809-07) and amplified by a fast preamp (Ortec 9306). The number of fluorescence photons per unit time, detected by the PMT, was always maintained to be less than 1% of the repetition rate of the excitation pulses. The TAC signal operated in reverse mode was sent to a multichannel analyzer (Oxford PCA3) placed

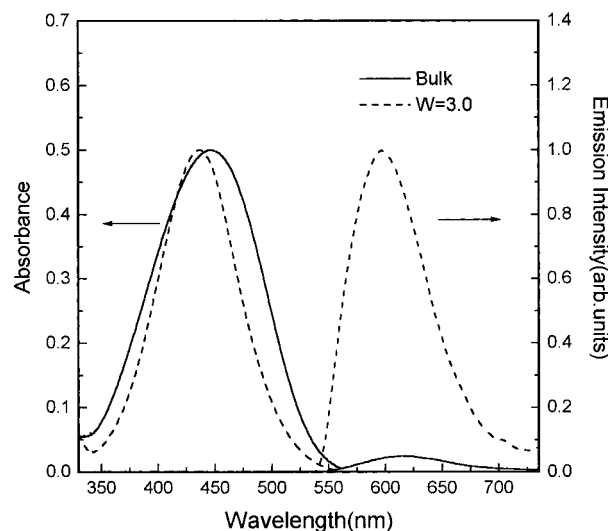


**Figure 2.** Absorption spectra and emission spectra of DASPI in bulk water and in an AOT reverse micelle ( $w = 3$ ).

in a computer. The maximum counts at the peak were higher than 30 000. The fwhm of the instrument response function obtained by a dilute solution of a silica sol was typically 50 ps. All the fluorescence decay times were measured at room temperature (23 °C). The true decay functions were extracted from the measured decay curves by deconvolution of the instrument response function using software capable of performing a four-exponential fitting. The quality of the fit was judged by the reduced  $\chi^2$  and by the autocorrelation function.

The absorption spectra were measured by a diode-array type multichannel detector, and the corrected emission spectra were measured by a spectrofluorometer (Hitachi F4500). DASPI and spectroscopic grade solvents were purchased from Aldrich. Aerosol OT (AOT, sodium bis(2-ethylhexyl) sulfosuccinate) was purchased from BDH Laboratory Supplies and purified by recrystallization from methanol and dried in vacuo at 50 °C. Doubly distilled water was used. The inclusion of DASPI in the reverse micelle was processed in the following way. An aqueous solution of DASPI and water was added to an *n*-heptane solution of AOT (0.1 M). The solution was agitated vigorously for 5 min with an automatic mixer. The water pool size was varied by changing the molar ratio of water/AOT. The concentration of DASPI in the solution was ca.  $10^{-5}$  M. This preparation method ensures that no more than one probe molecule is sequestered in a reverse micelle.

### Results and Discussion

**Steady-State Spectra.** Absorption and emission spectra of DASPI were measured in bulk water and in an AOT reverse micelle ( $w = 3$ ). As shown in Figure 2, the absorption maximum of DASPI in water occurs at 452 nm. The absorption spectrum of DASPI in the reverse micelle was largely blue-shifted, and its peak occurs at 435 nm. There is also a fair amount of reduction of the absorption bandwidth in the reverse micelle compared to that in bulk water. In general, most organic molecules having a TICT state show a red-shift in the absorption spectrum in more polar solvents. However, DASPI is unique in that its absorption spectrum is shifted to the blue in more polar solvents. Several attempts were made to provide an explanation for this unusual behavior. The vibrational frequency analysis of DASPI in various solutions revealed that there exist two resonance structures, the benzenoid and the quinoid forms.<sup>10</sup>

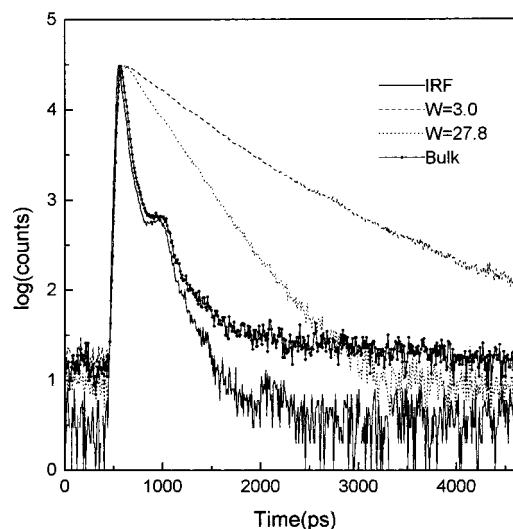
**TABLE 1: Absorption and Emission Characteristics of DASPI in AOT Reverse Micelles**

[H <sub>2</sub> O]/[AOT]	$\lambda_{\text{abs}}(\text{max})$ (nm)	$\lambda_{\text{em}}(\text{max})$ (nm)	fwhm (abs) (nm)	fwhm (em) (nm)
3.0	435	601	78	81
5.6	439	605	83	81
11.1	440	609	88	81
16.7	441	609	90	80
22.2	442	609	92	80
27.8	442	609	94	79
bulk	452	613	114	64

Depending on solvent polarity, DASPI favors one form over the other. In nonpolar solvents, the quinoid form is more stable, but in polar solvents the benzenoid form is more stable. As is previously known, the benzenoid form absorbs at a shorter wavelength than the quinoid form does.<sup>11</sup> In a reverse micelle, the absorption was shifted to the blue rather than to the red, despite the decrease of medium polarity. This can be understood by examining the microstructure of the reverse micelle. In the AOT micelle, the inner wall consists of sulfonate ionic groups. Since DASPI is dissolved as DASP<sup>+</sup> and I<sup>-</sup> in water, it is very likely that DASP<sup>+</sup> is located in the vicinity of the sulfonate group of the AOT molecule, and the Coulombic interaction will have an influence on the excited-state potential of DASPI. In the case of DASPI in the reverse micelle, this electrostatic effect on the absorption spectra dominates the medium polarity effect.

Table 1 shows the peak positions of the absorption and the emission spectra, together with their bandwidths as a function of the water pool size. The molar ratio of water to AOT, designated by  $w$ , was in the range 3–28. The radius of the water pool formed by the AOT reverse micelle is ca.  $2w$  in angstrom units. The  $w$  value of 3.0 has to be the lower limit, considering the size of DASPI. The upper limit of the water pool size ( $w = 27.8$ ) was chosen because the spherical shape could be destroyed at the higher water pool size.<sup>12</sup> It is seen that the absorption peak and the bandwidth increase with increasing micelle size. The absorption maximum was shifted to the red sharply up to the  $w$  value of 11.1 and shows virtually no change beyond the size. In contrast, the change of the emission maximum as well as the bandwidth is mild with increasing reverse micelle size. However, as shown in Figure 2, there is a huge increase in the fluorescence intensity. It has been known that the fluorescence quantum yield of DASPI rapidly decreases as the solvent polarity increases.<sup>3</sup> In aqueous solution, the fluorescence quantum yield of DASPI is known to be very low ( $\leq 0.001$ ).<sup>3</sup> To estimate the upper limit of the fluorescence lifetime in water, we have calculated the radiative decay rate from the absorption and the emission spectra using the Strickler–Berg formula.<sup>14</sup> The value of  $1.28 \times 10^8 \text{ s}^{-1}$  was obtained. Therefore, the fluorescence lifetime of DASPI in water should be approximately 10 ps. A simple comparison of the emission intensities in Figure 2 indicates that the lifetime of DASPI in the reverse micelle ( $w = 3$ ) should be higher than 200 ps. This estimation is meaningful only when the decay is monoexponential.

As was seen in Figure 2, the fluorescence intensity of DASPI confined in a reverse micelle was markedly increased, resulting from a decrease in the aniline motion that leads to a TICT state. Its dependence on the reverse micelle size is due to either the change of polarity or viscosity. The separation of the individual contributions may not be viable. The solvent polarity has an influence on the internal motion by affecting the excited-state potential. A quantum mechanical calculation showed that the barrier height for the internal twisting of DASPI increases as the medium becomes less polar. The solvent viscosity has an influence on the internal motion by the frictional force. In case

**Figure 3.** Fluorescence decay curves of DASPI in bulk water and in AOT reverse micelles.

of the reverse micelle, the medium viscosity increases as the reverse micelle size becomes smaller.

**Time-Resolved Studies.** Fluorescence lifetime measurements give direct information on dynamical rate processes. Figure 3 shows the fluorescence decay profiles at some selected water pools. The signal was detected at the maximum of the emission spectra. In bulk water, the fluorescence decay is very fast and close to the instrument response function. The nonlinear least-squares fitting accompanied by deconvolution gives a single-exponential decay time of DASPI in water of 11 ps with a reduced  $\chi^2$  value of 1.2. The time scale in fact is very close to the estimated value obtained from the steady-state spectra. As shown in Figure 3, the fluorescence emission of DASPI in the reverse micelle decays more slowly. In addition, the decay is not a single exponential. The same trend was also observed with other luminescing dyes in a water pool formed by a reverse micelle.<sup>14–16</sup> It has been inferred that the polarity heterogeneity (gradient) in the reverse micelle is responsible for the multiexponential decay.<sup>14</sup> The solvent polarity is the highest in the center and the lowest in the periphery region located in the vicinity of the inner wall of the AOT micelle. Because of this polarity gradient, the fluorescence emission decays multiexponentially in reverse micelles. We tried to fit the measured decay curves to a double-exponential form. All data were deconvoluted from the measured instrument function, and the obtained values were shown in Table 2. It is not possible to relate the double-decay components to the microstructure of the reverse micelle because it is very likely that the probe can move translationally through the heterogeneous region of the reverse micelle during the excited-state lifetime of the probe. The motion is not completely free but restricted by the micelle structure (spatial confinement) and by Coulombic interaction (electrostatic confinement). Another difficulty arises from the simultaneous change of both the lifetime components and their relative amplitudes when the reverse micelle size varies. What we need in this case is a single characteristic parameter that hopefully represents the molecular system having multiexponential decay components. For this purpose, the average lifetime has been commonly introduced as

$$\langle \tau \rangle = \alpha_1 \tau_1 + \alpha_2 \tau_2 \quad (1)$$

where  $\alpha$  and  $\tau$  are the amplitude and the decay time, respectively. The average lifetimes are also shown in Table 2. The

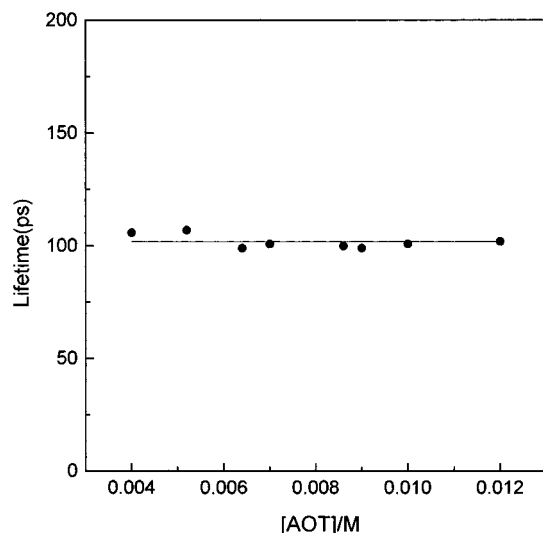


**Figure 4.** Fluorescence lifetimes of DASPI in AOT micelles as a function of the micelle concentration.

**TABLE 2: Fluorescence Decay Data of DASPI in AOT Reverse Micelles**

$w$	$A_1$	$\tau_1$ (ps)	$A_2$	$\tau_2$ (ps)	$\langle\tau\rangle$ (ps)	$\chi^2$
3.0	0.65	323	0.35	787	485	2.64
4.1	0.68	255	0.32	580	361	2.41
5.6	0.63	199	0.37	439	289	1.94
6.7	0.61	172	0.39	367	249	1.56
7.8	0.55	154	0.45	346	240	1.65
8.9	0.53	137	0.47	314	221	1.41
10.0	0.53	127	0.47	286	202	1.81
11.1	0.54	125	0.46	285	199	1.60
12.5	0.53	120	0.47	271	191	1.29
13.9	0.53	118	0.47	261	186	1.48
15.3	0.51	106	0.49	243	172	1.47
16.7	0.49	100	0.51	238	170	1.43
18.1	0.50	103	0.50	246	174	1.59
19.4	0.51	106	0.49	245	175	1.59
20.8	0.50	98	0.50	234	166	1.46
22.2	0.50	101	0.50	238	169	1.54
25.0	0.52	103	0.48	232	165	1.28
27.8	0.49	94	0.51	225	161	1.34

average decay times decrease from 485 to 161 ps as the reverse micelle size  $w$  increases from 3.0 to 27.8. Even at the highest  $w$ , the fluorescence lifetime is far larger than the value in bulk water. This is attributable to the strong attractive interaction between the probe and the ionic headgroup of the surfactant, the role of which was already revealed in the steady-state spectra. The effect of the attractive interaction between the probe and the AOT headgroup was examined by measuring the lifetime of DASPI in an aqueous micelle solution. In this normal micelle system, the probe solubilized in water should be located at the outside of the micelle where the polar ionic headgroup resides. Figure 4 shows the measured fluorescence lifetimes of DASPI as a function of the AOT concentration. The critical micelle concentration (cmc) of AOT at which the lifetime measurement starts has been known to be  $4 \times 10^{-3}$  M.<sup>17</sup> The fluorescence decay of DASPI in normal micelles exhibits two interesting features. One is that the measured lifetime of DASPI having a single decay time constant of ca. 100 ps is independent of the AOT concentration. The other is that the DASPI lifetime in the normal micelle approaches an asymptotic value in the reverse micelle system. In the reverse micelle, it is clear that the DASP cation is located in the vicinity of the sulfonate ion group, and thus, it can be stated that the strong interaction of DASP<sup>+</sup> with the sulfonate group influences the excited-state dynamics of the probe.

An important contribution of time-resolved laser spectroscopy to solution-phase dynamics is the direct measurement of the rotational time of small or medium-sized molecules.<sup>18</sup> It was frequently observed that the rotational motion does not follow the Stokes–Einstein law in two cases. One is the low-viscosity regime where the inertial motion dominates, and the other is when the sizes of the solute and the solvent are similar.<sup>19</sup> To overcome this problem, it was proposed that the effective friction be used, which can be obtained from the measured rotational correlation time.<sup>19,20</sup> In the Introduction, it was described that the most probable internal twisting of DSAPI is the rotation of the *N,N*-dimethylaniline moiety in aqueous solution. We wish to deduce the approximate time scale of the internal twisting motion from the rotational correlation time measurements. The overall rotational time of *N,N*-dimethylaniline and its analogues was previously measured by Hochstrasser and co-workers.<sup>21</sup> Aniline has its transition dipole moment along the short axis in the lowest electronic transition. The rotational time of *N,N*-dimethylaniline has been measured as 3.5 ps in methanol. Their results can be accommodated to explain our data because the twisting motion of the aniline moiety in DASPI is a rotation around the long axis. Assuming the molecular motion of DASPI follows the same hydrodynamic boundary condition (the sticky boundary condition, for example) in methanol and in water, the rotational time of *N,N*-dimethylaniline should amount to 6 ps in water at room temperature. This value is the upper limit of the fluorescence lifetime of DASPI in water when the internal twisting process is barrierless. Our fluorescence lifetime measurements for DASPI in water are similar to the estimated value, indicating that there is no appreciable barrier for the process. In fact, this is consistent with the result of a theoretical calculation.<sup>1</sup> The viscosity of a water pool in a reverse micelle is much larger than that of bulk water. By the steady-state anisotropy measurement, it was shown that the viscosity of the water pools in AOT reverse micelles is in the range 20–60 cP, using the Stokes–Einstein–Debye (SED) equation.<sup>17</sup> This means that the rotational correlation times in AOT reverse micelles would be 110–330 ps. This time scale is not very different from the fluorescence lifetimes measured in this work. It should be mentioned that applying the SED equation to the reverse micellar system needs some care. A recent time-resolved fluorescence anisotropy measurement showed that, in the case of the reverse micellar system, the overall motion of the reverse micelle as well as the wobbling motion of the probe must be taken into account, in addition to its tumbling motion in the reverse micelle.<sup>22</sup>

It seems that the increase of the water pool size shortens the fluorescence lifetime, resulting from both the polarity increase that lowers the potential barrier and the viscosity decrease that lowers the friction. Now we wish to relate the rate process for the internal twisting motion to the reverse micelle size. As already seen, the internal rotation of the aniline moiety is a major process that is responsible for the deactivation of the photoexcited DASPI. Therefore, its rate constant can be obtained from the nonradiative decay rate,  $k_{nr}$ , given by<sup>19</sup>

$$k_{nr} = 1/\langle\tau_F\rangle - k_r \quad (2)$$

where  $\langle\tau_F\rangle$  is the average lifetime and  $k_r$  the radiative decay rate. Figure 5 shows a plot of the nonradiative decay rate constant vs  $w$ . As seen in the figure, the internal twisting motion does not change monotonically as a function of the reverse micelle size. That is, up to the  $w$  value of 10, the rate increases rapidly and slows down beyond the size. An explanation for this trend can be inferred from the water pool nature enclosed in

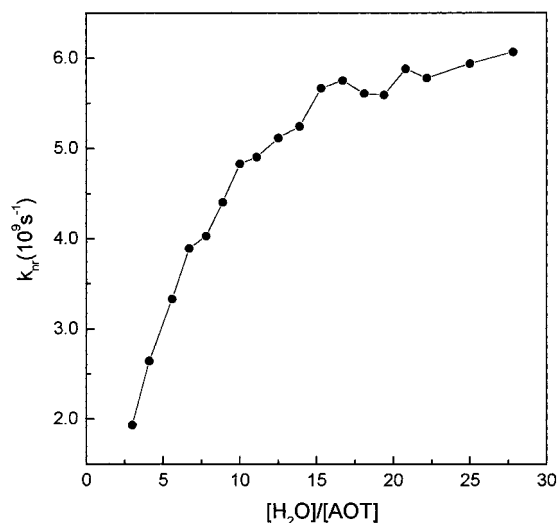


**Figure 5.** Nonradiative decay constants of the excited-state DASPI as a function of the water pool size.

the reverse micelle. A careful IR study confirmed that, in the reverse micelle having a size of  $w < 10$ , the water molecules exist as bound.<sup>23</sup> Above the size, the part of water located in the center becomes free. The fraction of the free water to the bound water increases as the water pool size increases. In accordance, the water polarity and viscosity change in a nonlinear fashion as the reverse micelle varies.

In solution phase, the rate processes of a large amplitude motion of a molecule are determined by the potential surface along the reaction coordinate and by solvent friction. The potential surface usually depends on the medium polarity. Although there have been several attempts to determine experimentally the polarity or dielectric constant of water pools confined in reverse micelles, they are either incomplete or qualitative.<sup>16,24,25</sup> Part of the difficulty arises from the fact that the dielectric constant is a macroscopic quantity, while the property of water nanoclusters should be understood on a microscopic level. Computer simulation may be a clue to solving the problem in that it already helped a lot in the understanding of the physical properties of "bulk water". The solvent friction exerted by a water nanocluster is more experimentally achievable than polarity. As mentioned previously, one way of obtaining it is to measure directly the overall rotational correlation time in the same environment. The obtained value through the Hubbard relation can be used to explain the viscosity dependence of the twisting motion of a molecule.<sup>20</sup> The method has been successfully applied to the large amplitude motion of stilbene and its analogues in hydrocarbon solvents.<sup>19,20</sup> Once the potential surface for the rate process is known as a function of the water pool size by any means, then the hydrodynamic theory can be applied to the molecular motion of DASPI in water nanoclusters.

Chemical reactions of a molecule in various sizes of solvent nanoclusters are an interesting topic. We intended to propose DASPI solvated in water nanoclusters as a model system for such a study and presented a series of experimental data on the rate processes. Although our observations were described on the grounds of the microstructure of water pools, some questions remain. It will be necessary to carry out further experimental and theoretical studies on the molecular motion of DASPI in water pools. The importance of this work, we believe, is in the attempt to obtain the time scale for the twisting molecular motion of a medium-sized molecule solvated in various sizes of water nanoclusters.

## Conclusion

This study concerns the influence of water solvents confined in a reverse micelle on the internal twisting dynamics of a photoexcited molecule. The excited-state lifetime of DASPI in bulk water has been measured as ca. 10 ps by the picosecond TCSPC system. When the molecule is solvated by a nanometer-sized water pool formed in an AOT reverse micelle, its fluorescence decay time markedly increases. This is attributable to a slow down of the internal twisting of DASPI in the AOT reverse micelle. The fluorescence decay dynamics of DASPI in reverse micelles having a size of 0.6–5.6 nm in radius exhibits a nonexponential nature, owing to the polarity heterogeneity of the water pool. The rate constant for the internal twisting of DASPI was obtained from the average lifetime of DASPI and decreases nonlinearly with increasing micelle size. It is concluded, albeit qualitatively, that the internal twisting motion of DASPI in water nanoclusters is significantly influenced by the micelle structure and solvent properties.

**Acknowledgment.** This work was financially supported by MOST through the Women's University Research Fund.

## References and Notes

- (1) Cao, X.; Tolbert, R. W.; McHale, J. L.; Edwards, W. D. *J. Phys. Chem. A* **1998**, *102*, 2739 and references therein.
- (2) Strehmel, B.; Seifert, H.; Rettig, W. *J. Phys. Chem. B* **1997**, *101*, 2232.
- (3) Gorner, H.; Gruen, H. *J. Photochem.* **1985**, *28*, 329.
- (4) Kumar, C. V.; Turner, R. S.; Asuncion, E. H. *J. Photochem. Photobiol. A* **1993**, *74*, 231.
- (5) Fromherz, P.; Heilemann, A. *J. Phys. Chem.* **1992**, *96*, 6864.
- (6) Eicke, H.-F.; Kvita, P. In *Reverse Micelles*; Luisi, P. L., Straub, B. E., Eds.; Plenum Press: New York, 1984; pp 29–35.
- (7) Eastoe, J.; Young, W. K.; Robinson, B. H. *J. Chem. Soc., Faraday Trans.* **1990**, *86*, 2883.
- (8) Fukazaki, M.; Miura, N.; Shiyasiki, N.; Kunita, D.; Shiyoya, S.; Haida, M.; Mashimo, S. *J. Phys. Chem.* **1995**, *99*, 431. (b) Bolton, P. S. *J. Phys. Chem.* **1995**, *99*, 17061.
- (9) Vajda, S.; Jimenez, R.; Rosenthal, S.; Fiddler, V.; Fleming, G. R.; Castner, E., Jr. *J. Chem. Soc., Faraday Trans.* **1995**, *91*, 867.
- (10) Tsukada, M.; Mineo, Y.; Itoh, K. *J. Appl. Phys.* **1989**, *93*, 7989.
- (b) Tsukada, M.; Mineo, Y.; Itoh, K. *J. Appl. Phys.* **1991**, *95*, 2451.
- (11) Shibasaki, K.; Itoh, K. *J. Raman Spectrosc.* **1991**, *22*, 753.
- (12) Huang, J. S.; Kotlarchyk, M.; Chen, S.-H. In *Micellar Solutions and Microemulsions*; Chen, S.-H., Rajagopalan, R., Eds.; Springer-Verlag: New York, 1990; pp 227–249.
- (13) Strickler, S. J.; Berg, R. A. *J. Chem. Phys.* **1962**, *37*, 814.
- (14) Cho, C. H.; Chung, M.; Lee, J.; Nguyen, T.; Singh, S.; Vedamuthu, M.; Yao, S.; Zhu, J.-B.; Robinson, G. W. *J. Phys. Chem.* **1995**, *99*, 7806.
- (15) Sarkar, N.; Das, K.; Datta, A.; Das, S.; Bhattacharyya, K. *J. Phys. Chem.* **1996**, *100*, 10523.
- (16) Datta, A.; Mandal, D.; Pal, S. K.; Bhattacharyya, K. *J. Phys. Chem. A* **1997**, *101*, 3299.
- (17) Hasegawa, M.; Sugimura, T.; Suzuki, Y.; Shindo, Y.; Kitahara, A. *J. Phys. Chem.* **1994**, *98*, 2120.
- (18) Fleming, G. *Chemical Applications of Ultrafast Spectroscopy*; Oxford University Press: New York, 1986.
- (19) Lee, M.; Bain, A. J.; McCarthy, P. J.; Han, C. H.; Haseltine, J. N.; Smith, A. B., III; Hochstrasser, R. M. *J. Chem. Phys.* **1986**, *85*, 4341.
- (20) Velsko, S. P.; Waldeck, D. H.; Fleming, G. R. *J. Chem. Phys.* **1983**, *78*, 249.
- (21) Myers, A. B.; Pereira, M. A.; Holt, P. L.; Hochstrasser, R. M. *J. Chem. Phys.* **1987**, *86*, 5146.
- (22) Wittouck, N.; Negri, R. M.; Ameloot, M.; De Schryver, F. C. *J. Am. Chem. Soc.* **1994**, *116*, 10601.
- (23) Jain, T. K.; Varshney, M.; Maitra, A. *J. Phys. Chem.* **1989**, *93*, 7409.
- (24) Belletete, M.; Lachapelle, M.; Durocher, G. *J. Phys. Chem.* **1990**, *94*, 5337.
- (25) Hof, M.; Lianos, P.; Laschewsky, A. *Langmuir* **1997**, *13*, 2181.